diabetes®
American Diabetes Association®

Antihypertensive Drug Amlodipine Besylate Shows Potential in Alleviating Diabetic Peripheral Neuropathy

Yuxi Wei, Yujie Huang, Runzhi Huang, Yuan Ruan, Tian Feng, Fan Zhou, Wei Zhang, Jianyu Lu, Sujie Xie, Yuntao Yao, Jiaying Wang, Shizhao Ji, and Xu Shen

Diabetes 2025;74(6):983–997 | https://doi.org/10.2337/db24-0403

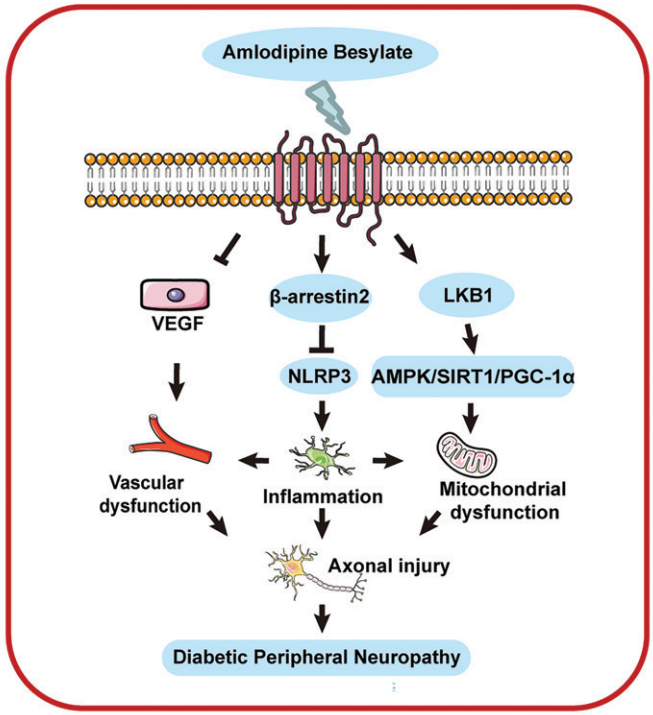

Schematic summary of the mechanism underlying the amelioration of amlodipine besylate on diabetic peripheral neuropathy in mice. Amlodipine besylate as a GPR40 agonist ameliorated diabetic peripheral neuropathy-like pathology in mice with both type 1 diabetes and type 2 diabetes. Amlodipine besylate suppressed inflammation by regulating the GPR40/β-arrestin2/NLRP3 pathway in sciatic nerves and improved mitochondrial dysfunction through the GPR40/LKB1/AMPK/SIRT1/PGC-1α pathway in sciatic nerves and DRG tissues.

Antihypertensive Drug Amlodipine Besylate Shows Potential in Alleviating Diabetic Peripheral Neuropathy

Yuxi Wei,[1] Yujie Huang,[1] Runzhi Huang,[2] Yuan Ruan,[1] Tian Feng,[1] Fan Zhou,[1] Wei Zhang,[2] Jianyu Lu,[2] Sujie Xie,[2] Yuntao Yao,[2] Jiaying Wang,[1] Shizhao Ji,[2] and Xu Shen[1,3]

Diabetes 2025;74:983–997 | https://doi.org/10.2337/db24-0403

Diabetic peripheral neuropathy (DPN) is a common diabetes complication with no currently available curative treatments. Here, we demonstrated that the protein level of G-protein–coupled receptor 40 (GPR40) is significantly repressed in the sciatic nerves (SNs) of DPN patients, as well as in the peripheral nerves, including dorsal root ganglia (DRG) and SNs, of streptozotocin-induced type 1 diabetic mice and BKS Cg-m$^{+/+}$*Lepr db*/*J* (*db*/*db*) type 2 diabetic mice. We identified that amlodipine besylate (AB), a first-line clinical antihypertensive drug, is a GPR40 agonist capable of alleviating DPN-like pathologies in mice. These pathologies include neurological damage, destruction of myelin sheath structures, vascular injury, loss of intraepidermal nerve fibers, and impaired neurite outgrowth in DRG neurons. To elucidate the underlying mechanisms, we generated the DPN mice with GPR40-specific knockdown in SN and DRG tissues using adeno-associated virus 8-*GPR40-RNAi*. Mechanistically, AB attenuated inflammatory responses via the GPR40/β-arrestin2/NLRP3 pathway and ameliorated mitochondrial dysfunction through the GPR40/LKB1/AMPK/SIRT1/PGC-1α pathway in DPN mice, which were all further validated in primary human Schwann cells. Additionally, AB suppressed the cross talk between Schwann cells and endothelial cells/DRG neurons in DPN mice. Collectively, our findings highlight the potential of AB for the treatment of DPN.

ARTICLE HIGHLIGHTS

- The antihypertensive drug amlodipine besylate (AB) is a novel G-protein–coupled receptor 40 agonist able to ameliorate diabetic peripheral neuropathy (DPN)-like pathologies in mice.
- AB represses inflammation, apoptosis, and mitochondrial dysfunction in DPN mice.
- AB suppressed the cross talk between Schwann cells and endothelial cells/dorsal root ganglia neurons.
- AB shows potential in treating late-stage DPN.

Diabetic peripheral neuropathy (DPN) is a prevalent and debilitative diabetes complication, severely impacting the life quality of the patients. In the late-stage of DPN, patients often experience clinical symptoms such as numbness, allodynia, and sensory loss in their limbs (1). However, these symptoms are frequently overlooked until the foot ulcers develop. Once the foot ulcers appear, they are notoriously difficult to heal, with ∼20% of diabetic foot infections leading to varied degrees of amputation (2). Although surgical interventions can alleviate some symptoms, the underlying neuropathy remains unresolved and is prone to recurrence. Notably, glycemic control can mitigate early-stage DPN symptoms but offers no significant beneficial effects in the late stage (3–5). To date, there are no curative treatments for DPN, due to the limited understanding of its complex pathogenesis.

Pathologically, DPN involves axonal degeneration, demyelination, and the accumulation of extracellular matrix proteins, all of which contribute to the irreversible nerve damage (2). Multiple risk factors are implicated in the progression of DPN, including neuroinflammation (6), oxidative

[1]Jiangsu Key Laboratory of Drug Target and Drug for Degenerative Diseases, School of Medicine, Nanjing University of Chinese Medicine, Nanjing, China
[2]Department of Burn Surgery, the First Affiliated Hospital of Naval Medical University, Shanghai, China
[3]State Key Laboratory on Technologies for Chinese Medicine Pharmaceutical Process Control and Intelligent Manufacture, Nanjing University of Chinese Medicine, Nanjing, China

Corresponding author: Xu Shen, xshen@njucm.edu.cn, Shizhao Ji, shizhaoji2022@163.com, or Jiaying Wang, wangjy@njucm.edu.cn

Received 13 May 2024 and accepted 26 February 2025

This article contains supplementary material online at https://doi.org/10.2337/figshare.28500470.

Y.W., Y.H., and R.H. contributed equally.

stress (7), mitochondrial dysfunction (8), and bioenergetic crisis (9). For example, elevated levels of proinflammatory cytokines, such as interleukin-1β (IL-1β), have been detected in plasma of DPN patients (6), accompanied by an accumulation of activated $CD68^+$ macrophages in sciatic nerves (SNs) (10) and depolarization of the mitochondrial membrane potential in sensory neurons of diabetic mice (8).

G-protein–coupled receptor 40 (GPR40) is a seven-transmembrane protein widely expressed in the central nervous system (11) and peripheral nervous system, including dorsal root ganglia (DRG) and SN tissues (12). Activation of GPR40 has been shown to regulate neuroinflammation (13), cell apoptosis (14), mitochondrial dysfunction (15), and energy metabolic disorders (16), all of which are closely associated with DPN pathology (17). In addition, we have also previously reported the potential beneficial effects of GPR40 activation in alleviating DPN-like pathology in mice, although clinical validation remains lacking (12).

Motivated by these findings, we recently conducted a study to explore and functionally characterize novel GPR40 activators, aiming to elucidate their underlying mechanisms against DPN using clinical samples from DPN patients. This work provides a foundation for the discovery of druggable anti-DPN lead compounds.

In our search for GPR40 activators, we screened the laboratory in-house U.S. Food and Drug Administration–approved compound library using our previously established screening platform (18). Through this process, amlodipine besylate (AB) (Fig. 1*I*), a first-line clinical antihypertension drug, was determined as a GPR40 agonist. Published reports indicated that AB exhibits neuroprotection (19,20), anti-inflammation (21), and antioxidative stress effects (20). These properties prompted us to investigate its potential in amelioration of DPN pathology.

Cellular communications function potently in the molecular mechanisms underlying many diseases by regulating metabolism, energy transformation, immune responses, and other critical functions of organisms (22). In DPN pathology, cellular communication within the dynamic interplay of multiple cell types in peripheral nerve tissues is intricately involved in the regulation of inflammation and myelin sheath injury (23–26).

In the current study, we demonstrated that GPR40 protein levels are pathologically downregulated in the SN tissues of DPN patients as well as in the DRG and SN tissues of streptozotocin (STZ)-induced type 1 diabetic mice and BKS Cg-$m^{+/+}$*Lepr db/J* (*db/db*) type 2 diabetic mice. We identified AB as a potent GPR40 agonist that efficiently ameliorated DPN-like pathology in mice. To elucidate the underlying mechanisms, the DPN mice with GPR40-specific knockdown were generated by injection of the adeno-associated virus (AAV) 8-*GPR40-RNAi*. Furthermore, we explored the cellular communications between Schwann cells and endothelial cells/DRG neurons in the DPN model mice using AB as a molecular probe. Our findings strongly support that pharmacological activation of GPR40 as a promising therapeutic strategy for DPN and highlight the potential of AB in treating this disease.

RESEARCH DESIGN AND METHODS

Animals

The type 1 diabetic mice model was prepared by intraperitoneal injection of STZ (150 mg/kg) into 8-week-old male C57BL/6 mice. Diabetic mice were defined by the glycemic value of >16 mmol/L (288 mg/dL), and the type 1 diabetic mice with late-stage DPN were evaluated by assessing the DPN-like pathological behaviors. (Protocols were approved by the Institutional Animal Care and Use Committees at Nanjing University of Chinese Medicine. Ethical approval no. 202007A027.)

The 18-week-old male *db/db* mice were verified as type 2 diabetic mice with late-stage DPN (27,28), and age-matched heterozygotes mice (*db/m*) were included as control mice in *db/db* mice-related assays. (Protocols were approved by the Institutional Animal Care and Use Committees at Nanjing University of Chinese Medicine. Ethical approval no. 202103A019.)

STZ mice were injected with AAV8-*GPR40-RNAi* or AAV8-*NC-RNAi* to tibialis anterior and gastrocnemius muscles (1.1×10^{11} viral genomes), and knockdown efficiency was detected 2 weeks after AAV8 injection (Supplementary Fig. 7*C* and *D*). (Protocols were approved by the Institutional Animal Care and Use Committees at Nanjing University of Chinese Medicine. Ethical approval no. 202103A013.)

The specific protocols can be found in the Supplementary Material.

Statistical Analysis

All data are expressed as mean ± SEM and were analyzed by GraphPad Prism 9.0 software. The unpaired two-tailed Student *t* test was used for two-group comparison. Student *t* test, one-way ANOVA with the Dunnett post hoc test and two-way ANOVA with the Bonferroni post hoc test were used for comparisons of at least three groups. $P < 0.05$ was considered statistically significant.

Data and Resource Availability

The data supporting the findings are available from the corresponding authors upon reasonable request.

RESULTS

GPR40 Expression Was Pathologically Downregulated in the SN and DRG Tissues of DPN Mice and Patients

DPN Mice

Immunostaining (Fig. 1*A–D*) and quantitative real-time PCR (Fig. 1*E* and *F*) results indicated that both the protein and mRNA levels of GPR40 were repressed in the SN and DRG tissues of DPN mice (STZ, *db/db*).

DPN Patients

Additionally immunostaining results also demonstrated that GPR40 protein level was suppressed in the SN of DPN

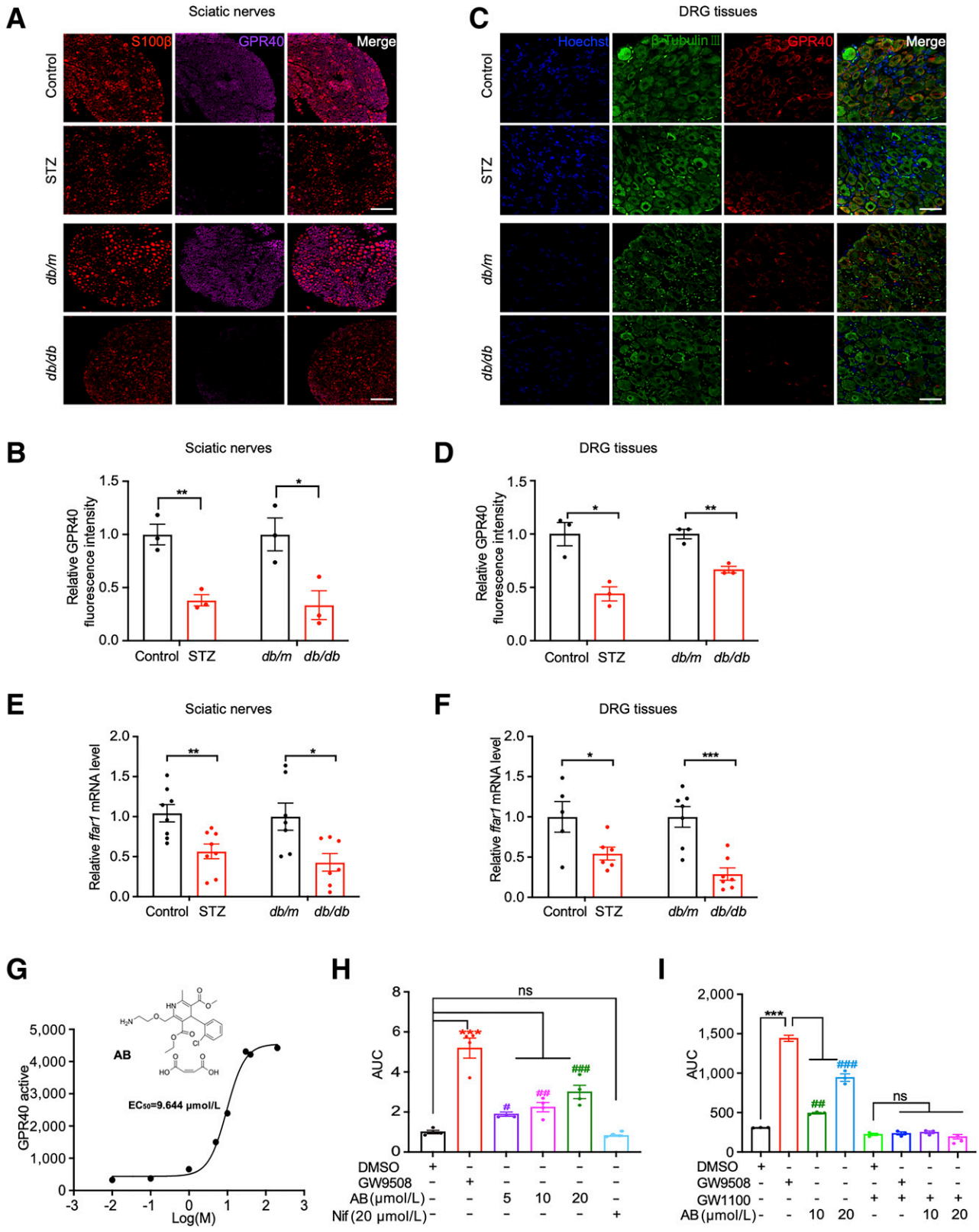

Figure 1—GPR40 expression was pathologically downregulated in SNs and DRG tissues of DPN mice. *A–D*: Immunofluorescence with quantification results demonstrated that the protein level of GPR40 (purple, red) was reduced in SNs and DRG tissues from DPN mice (STZ, *db/db*; $n = 3$). Scale bar: 25 μm. *E* and *F*: Real-time PCR results revealed that the mRNA level of *ffar1* was decreased in SNs and DRG tissues from DPN mice (STZ, $n = 8$; *db/db*, $n = 6$). *G*: Structure of AB and its EC_{50} value for evaluation of the capability on GPR40 activation. *H*: GW9508 (a known GPR40 agonist, 10 nmol/L), Nifedipine (a known calcium antagonist, 20 μmol/L) or AB (5, 10, and 20 μmol/L) activated GPR40 in the GPR40-overexpressed CHO cells ($n = 4$). *I*: GW9508 (10 nmol/L) or AB (5, 10, and 20 μmol/L) lost its excitatory effect on GPR40 in the presence of GW1100 (a known GPR40 inhibitor, 10 μmol/L) in the GPR40-overexpressed CHO cells ($n = 3$). AUC, area under the curve. All values are presented as mean ± SEM. $^*P < 0.05$, $^{**}P < 0.01$, $^{***}P < 0.001$, #$P < 0.05$, ##$P < 0.01$, ###$P < 0.001$; one-way ANOVA with the Dunnett post hoc test.

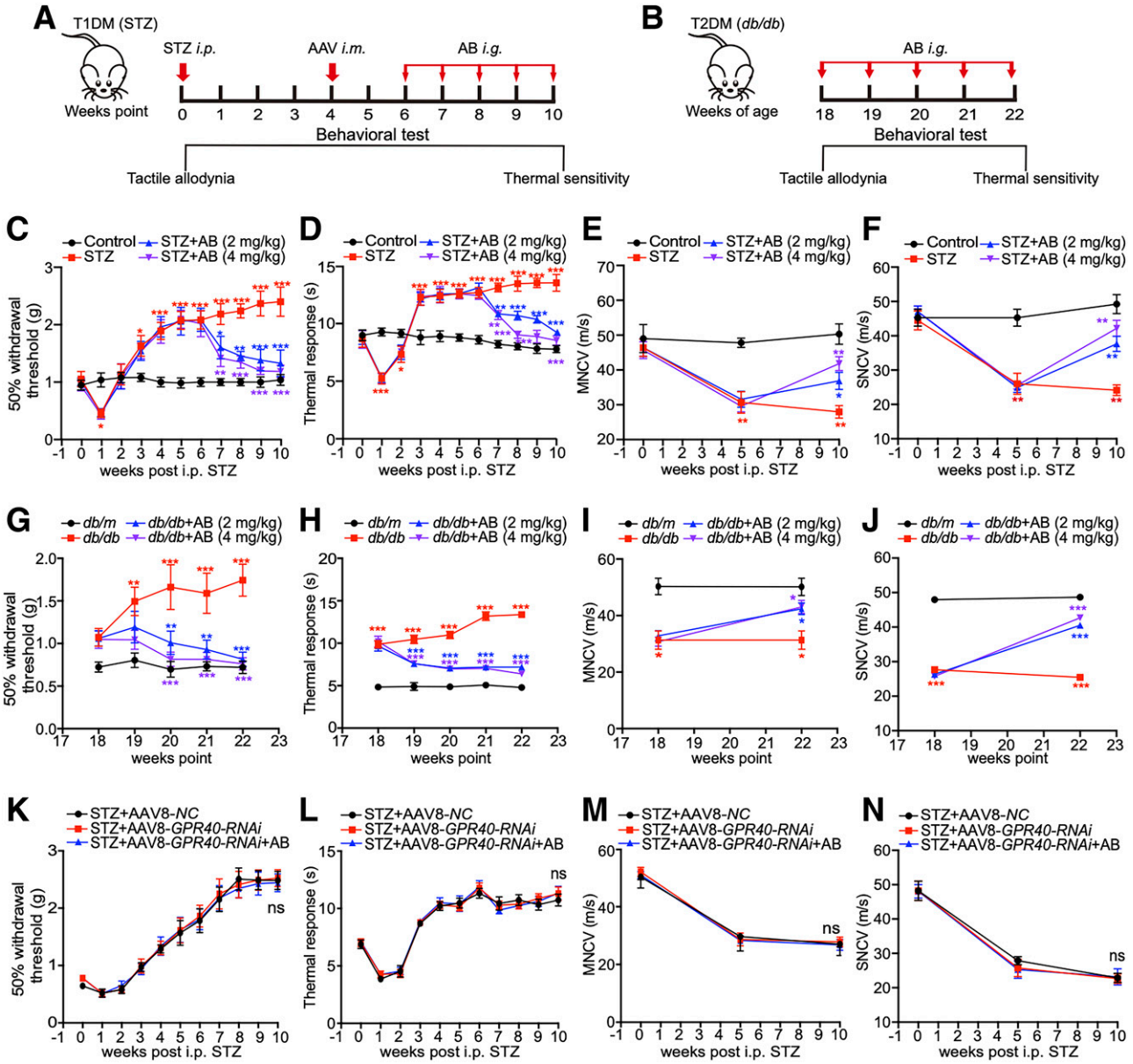

Figure 2—AB ameliorated nerve dysfunction and peripheral nerve injury in DPN mice targeting GPR40. *A* and *B*: Schedule for animal experimental for DPN mice (STZ and *db/db*). STZ mice (6 weeks after STZ injection) and *db/db* mice (18 weeks old) were treated with AB (2 or 4 mg/kg/day) for 4 weeks. i.p., intraperitoneal; T1DM, type 1 diabetes mellitus; T2DM, type 2 diabetes mellitus; i.g., intragastric. AAV8-*GPR40-RNAi* was intramuscularly (i.m.) injected to STZ mice or *db/db* mice 2 weeks before AB administration. AB (2 or 4 mg/kg/day) reduced mechanical response latency (Von Frey test) (*C* and *G*) and thermal response latency (Plantar test) (*D* and *H*), and improved motor nerve conduction velocity (MNCV) in DPN mice (STZ, $n = 12$; *db/db*, $n = 8$) (*E* and *I*). *F* and *J*: AB (2 or 4 mg/kg/day) improved slow sensory nerve conduction velocity (SNCV) of DPN mice (STZ, $n = 12$; *db/db*, $n = 8$). *K*–*N*: AB (4 mg/kg/day) had no impacts on nerve functions in the AAV8-*GPR40-RNAi*–injected STZ mice ($n = 12$). All values are presented as mean ± SEM. *$P < 0.05$, **$P < 0.01$, ***$P < 0.001$, two-way ANOVA with Bonferroni post hoc test.

patients compared with normal individuals (Supplementary Fig. 1*A*).

These results indicated the potential regulation of GPR40 against the late-stage DPN pathology.

AB Was an Agonist of GPR40

Given the pathological repression of GPR40 in DPN mice, we proposed that pharmacological activation of GPR40 might ameliorate the DPN-like pathology in mice (12). Thus, the in-house laboratory compound library was searched for GPR40 agonists, and AB (Fig. 1*G*) was finally determined to be a potential agonist of GPR40 by the constructed platform (18). It promoted Ca^{2+} release from the endoplasmic reticulum and induced a transient change of Ca^{2+} flow in CHO cells that stably overexpress human-GPR40 (hGPR40-CHO).

As indicated in Fig. 1*G* and *H*, AB activated GPR40 in hGPR40-CHO cells with an EC_{50} value of 9.644 μmol/L. Given that AB is also a calcium-channel blocker, additional

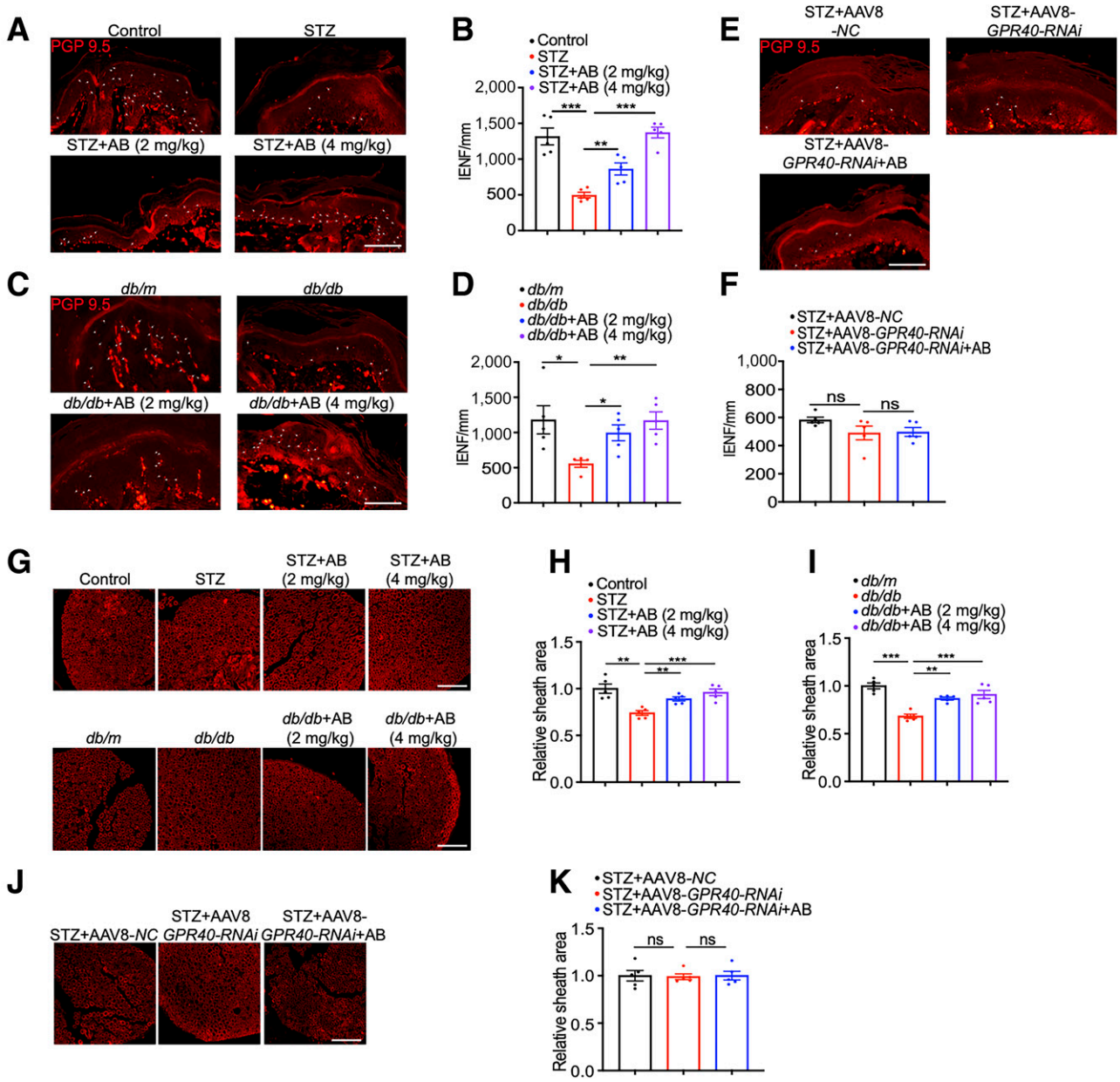

Figure 3—AB ameliorated IENF density and myelin sheath injury in DPN mice targeting GPR40. *A–F*: Immunofluorescence (PGP 9.5-labeled IENFs, red) with quantification results suggested that AB (2 or 4 mg/kg/day) improved the IENFs loss in foot pads from DPN mice (STZ, $n = 5$; *db/db*, $n = 5$) (*A–D*), while AB (4 mg/kg/day) rendered no effects on IENFs loss in the AAV8-*GPR40-RNAi*–injected STZ mice ($n = 5$) (*E* and *F*). *G–K*: Immunofluorescence (myelin basic protein-labeled myelin sheath, red) with quantification results showed that AB (2 or 4 mg/kg/day) increased the area of myelin sheath in sciatic nerves from DPN mice (STZ, $n = 5$; *db/db*, $n = 5$) (*G–I*), while AB (4 mg/kg/day) had no effects on myelin sheath area in the AAV8-*GPR40-RNAi*–injected STZ mice ($n = 5$) (*J* and *K*). Scale bar: 25 μm. All values are presented as mean ± SEM. $^*P < 0.05$, $^{**}P < 0.01$, $^{***}P < 0.001$; ns, not significant; one-way ANOVA with the Dunnett post hoc test.

assays were also done to exclude the possibility that AB activated GPR40 by its inhibition against calcium channels in hGPR40-CHO cells. As we expected, the results demonstrated that nifedipine as a calcium-channel blocker antihypertension drug failed to activate GPR40 (Fig. 1*H*) and that the selective GPR40 antagonist GW1100 (13) deprived AB of its capability in activating GPR40 (Fig. 1*I*). All results demonstrated that AB was an agonist of GPR40.

AB Ameliorated Nerve Dysfunctions in DPN Mice by Targeting GPR40

We next examined the potential of AB as a GPR40 activator in ameliorating the nerve dysfunctions in DPN mice (STZ, *db/db*) (29). Schematics of the animal assays are shown in Fig. 2*A* and *B*.

The results revealed that DPN mice (STZ, *db/db*) displayed a series of DPN-like pathologies such as aggravated 50% paw withdrawal threshold (Fig. 2*C* and *G*), prolonged

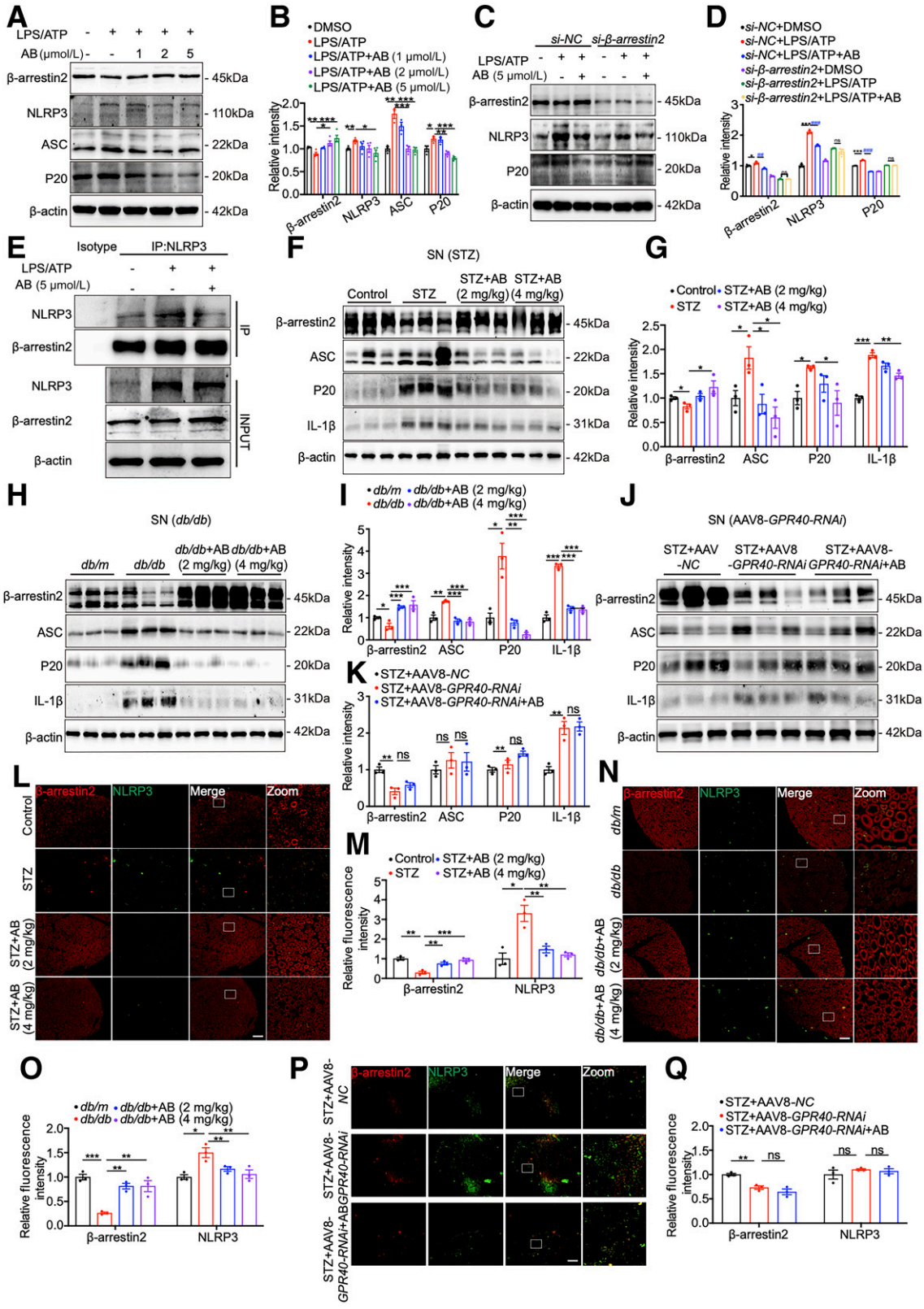

Figure 4—AB suppressed neuroinflammation through the GPR40/β-arrestin2/NLRP3 pathway. *A* and *B*: Western blot with quantification results demonstrated AB (1, 2, or 5 μmol/L) increased the protein levels of GPR40 and β-arrestin2 and reduced the protein levels of NLRP3, ASC and P20 in LPS (1 μg/mL)/ATP (3 mmol/L)-treated RSC96 cells ($n = 3$). *C* and *D*: Western blot with quantification results indicated that AB (5 μmol/L) had no effects on NLRP3 inflammasome-related protein levels in LPS/ATP-treated RSC96 cells with *si-β-arrestin2* transfected ($n = 3$). *E*: Immunoprecipitation assay results indicated that AB (5 μmol/L) increased the interaction between NLRP3 and β-arrestin2. *F–I*: Western blot with quantification results suggested that AB (2 or 4 mg/kg/day) increased the protein level of

thermal response latency (Fig. 2*D* and *H*), tardy motor nerve conduction velocity (Fig. 2*E* and I), and delayed sensory nerve conduction velocity (Fig. 2*F* and *J*). Obviously, AB ameliorated all above-mentioned nerve dysfunctions in DPN mice (Fig. 2*C–J*) but lost those beneficial effects in AAV8-*GPR40-RNAi*–injected DPN mice (Fig. 2*K–N*).

Additionally, AB had no impacts on blood glucose, body weight, or insulin levels in DPN mice, possibly due to the serious metabolic abnormalities and very high level of glucose in the late stage of DPN (Supplementary Fig. 1*B–G*, *L*, and *M*). Moreover, AB also had no influence on nerve functions or blood glucose in nondiabetic mice (Supplementary Fig. 1*H–K*).

All results demonstrated that AB ameliorated nerve dysfunctions in DPN mice targeting GPR40.

AB Improved Intraepidermal Nerve Fibers Loss and Myelin Sheath Structural Damage in DPN Mice Targeting GPR40

AB Upregulated Intraepidermal Nerve Fibers Density in DPN Mice by Targeting GPR40

The intraepidermal nerve fibers (IENFs) density was detected using PGP9.5 (10). The results indicated that AB upregulated the IENFs density in DPN mice but had no impacts on the IENFs density in AAV8-*GPR40-RNAi*–injected DPN mice (Fig. 3*A–F*).

AB Protected Against SN Myelin Sheath Structural Damage in DPN Mice by Targeting GPR40

The potential amelioration of AB on SN myelin sheath damage was detected by immunofluorescence-based staining myelin basic protein (30) and Luxol fast blue staining (31). The results indicated that DPN mice (STZ, *db/db*) had a thinner myelin sheath thickness and displayed a sparse, disorganized arrangement of myelin sheaths in the SN tissues, while AB treatment ameliorated such damage by showing thicker and tight arrangement in DPN mice. Notably, AB lost such an ameliorative effect in AAV8-*GPR40-RNAi*–injected DPN mice (Fig. 3*G–K* and Supplementary Fig. 2*A–C*).

All results demonstrated that AB improved intraepidermal nerve fibers loss and protected against SN myelin sheath structural damage in DPN mice by targeting GPR40.

AB Suppressed Neuroinflammation Through the GPR40/β-Arrestin2/NLRP3 Pathway

In the peripheral nervous system, Schwann cells are the most prevalent glial cells wrapping around axons for physical support and act as the first response cells by releasing varied signaling factors for interaction with the other cells (32). Schwann cells injury and Schwann cells-mediated inflammation are tightly involved in DPN pathology (33), and immunofluorescence results indicated that inflammatory-related protein NLRP3 was predominantly expressed in Schwann cells (Fig. 1*A* and *B* and Supplementary Fig. 2*D–F*). Thus, Schwann cells were used to assess inflammatory response in the current work.

AB Suppressed Neuroinflammation Through Lipopolysaccharide/ATP-Treated Schwann Cells via the GPR40/β-Arrestin2/NLRP3 Pathway

NLRP3 inflammasome is a multiprotein complex composed of sensor molecule NLRP3, adaptor protein ASC, and cleaved caspase 1 (P20), while its activation promotes IL-1β into a mature form initiating inflammation progression. The processing and release of IL-1β from NLRP3 inflammasome were promoted in DPN mice (33).

We here used lipopolysaccharide (LPS) and ATP to simulate an acute inflammatory response in vitro (34). Western blot results indicated that AB antagonized the LPS/ATP-induced increases in NLRP3, ASC, and P20 (Fig. 4*A* and *B*), indicative of the suppression of inflammation in RSC96 cells. Considering the long-term hyperglycemic environment in DPN pathology, we investigated whether high glucose (HG) might induce inflammatory response in vitro. The immunofluorescence results indicated that HG (250 mmol/L) treatment for 48 h also induced an inflammatory response in RSC96 cells as indicated by the upregulated expression levels of NLRP3 and ASC, and AB treatment antagonized such a HG-induced inflammatory response (Supplementary Fig. 3*A–C*). However, due to the inherent instability of HG, we opted to use the well-established LPS/ATP inflammatory model for the mechanistic investigations (12,34).

β-Arrestin2, as a scaffold protein of GPR40, is tightly linked to NLRP3 inflammasome activation (35), and our results demonstrated that AB antagonized the LPS/ATP-induced decreases in β-arrestin2 and GPR40 (Fig. 4*A* and *B*). Then, we explored the role of β-arrestin2 in the AB-mediated regulation against NLRP3 inflammasome. As indicated in Fig. 3*C* and *D*, *si-β-arrestin2* deprived AB of its capability in antagonizing NLRP3 inflammasome-related proteins expression in LPS/ATP-treated RSC96 cells.

Meanwhile, β-arrestin2 suppressed the assembling of NLRP3 inflammasome (35), and our coimmunoprecipitation results revealed that NLRP3 could pull down β-arrestin2 in

β-arrestin2 but decreased the protein levels of ASC, P20, and IL-1β in SNs from DPN mice (STZ, $n = 3$; *db/db*, $n = 3$). *J* and *K*: Western blot with quantification results demonstrated that AB (4 mg/kg/day) had no effects on β-arrestin2/NLRP3 signaling in AAV8-*GPR40-RNAi*–injected DPN mice (STZ, $n = 3$; *db/db*, $n = 3$). Immunofluorescence with quantification results indicated that AB (2 or 4 mg/kg/day) upregulated the expression of β-arrestin2 (red) but downregulated the expression of NLRP3 (green) in DPN mice (STZ, $n = 3$; *db/db*, $n = 3$) (*L–O*), while AB (4 mg/kg/day) had no impacts on the expression of β-arrestin2 and NLRP3 in SNs from AAV8-*GPR40-RNAi*–injected STZ mice ($n = 3$) (*P* and *Q*). Scale bar: 25 μm. All values are presented as mean ± SEM. *$P < 0.05$, **$P < 0.01$, ***$P < 0.001$, ##$P < 0.01$, ###$P < 0.001$; ns, not significant; one-way ANOVA with the Dunnett post hoc test.

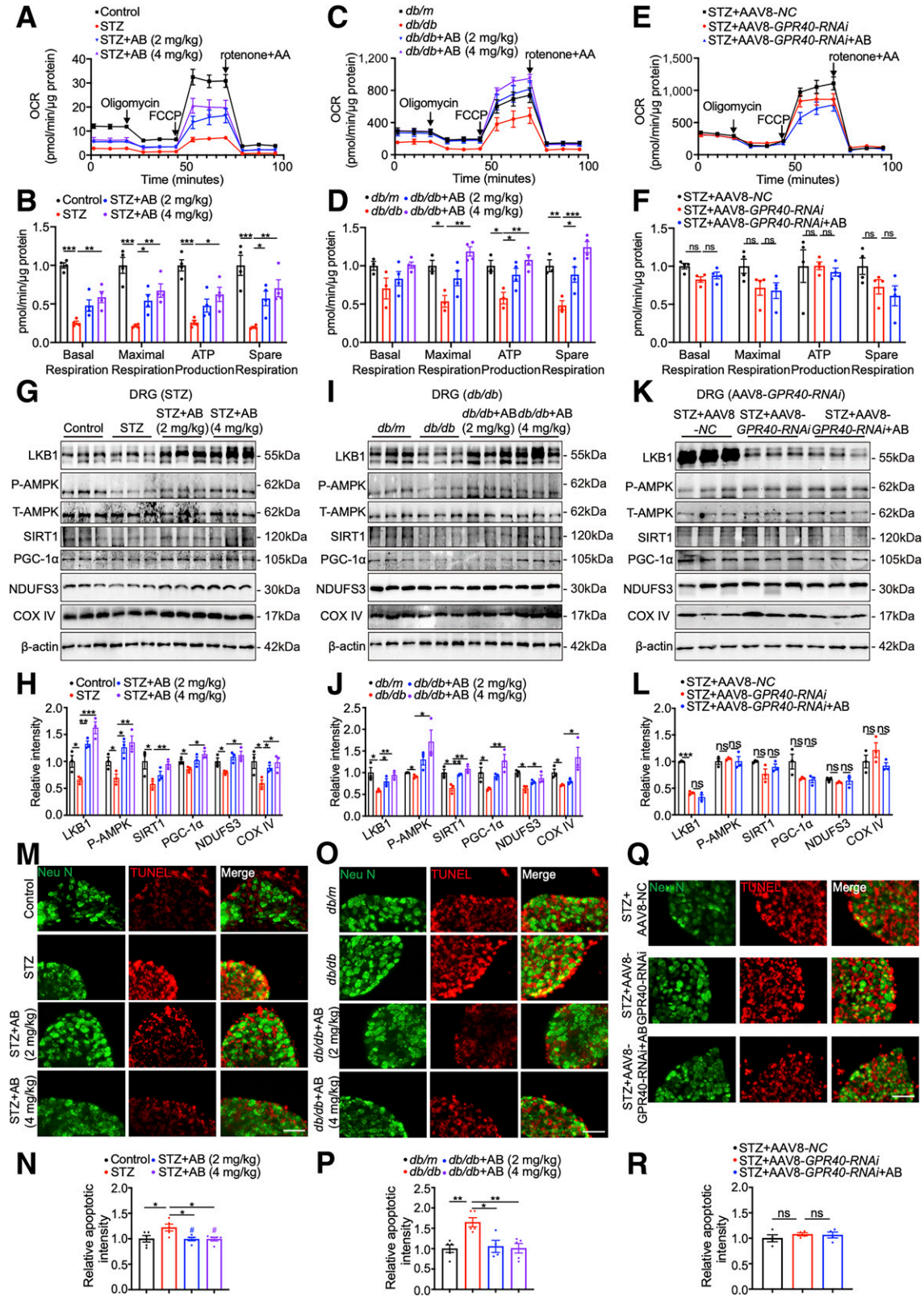

Figure 5—AB protected against DRG neuronal apoptosis and mitochondrial dysfunction through the GPR40/LKB1/AMPK/SIRT1/PGC-1α pathway. *A* and *C*: OCR of DRG neurons isolated from DPN mice were measured at the basal level and the sequential addition of oligomycin (1 μmol/L), carbonylcyanide-4-(trifluoromethoxy)-phenylhydrazone (FCCP) (1 μmol/L) and the mixture of rotenone/antimycin A (1 μmol/L). Data are expressed as OCR in pmol/min/μg protein normalized to total protein in each well. *B* and *D*: AB (2 or 4 mg/kg/day) improved basal respiration, maximal respiration, ATP production, and spare respiration capacity in DRG neurons from DPN mice (STZ, $n = 4$; *db/db*, $n = 4$). *E* and *F*: AB (4 mg/kg/day) failed to enhance OCR, basal respiration, maximal respiration, ATP production, and spare

LPS/ATP-treated RSC96 cells, indicative of the binding of β-arrestin2 to NLRP3, and AB enhanced the β-arrestin2/NLRP3 binding (Fig. 4*E*).

Therefore, all results demonstrated that AB suppressed neuroinflammation in RSC96 cells via the GPR40/β-arrestin2/NLRP3 pathway.

AB Repressed Neuroinflammation of SNs in DPN Mice Through the GPR40/β-Arrestin2/NLRP3 Pathway

Western blot and immunofluorescence results both indicated that AB upregulated the protein level of β-arrestin2 and downregulated the protein levels of NLRP3, ASC, P20, and IL-1β (Fig. 4*F–I* and *L–O*). Meanwhile, immunofluorescence results demonstrated that β-arrestin2 and NLRP3 were co-located in SNs, supporting the binding of β-arrestin2 with NLRP3 in the suppression of the inflammatory response (Fig. 4*L–O*). Notably, AB had no impacts on the GPR40/β-arrestin2/NLRP3 pathway in AAV8-*GPR40-RNAi*–injected DPN mice (Fig. 4*J, K, P*, and *Q*).

Together, all results demonstrated that AB suppressed neuroinflammation in DPN mice through the GPR40/β-arrestin2/NLRP3 pathway.

AB Protected Against DRG Neuronal Apoptosis and Mitochondrial Dysfunction Through the GPR40/LKB1/AMPK/SIRT1/PGC-1α Pathway

Mitochondrial dysfunction leads to axonal degeneration, and DRG neuronal apoptosis is a hallmark of DPN (9). Here, we inspected the beneficial effects of AB on mitochondrial function.

AB Improved Mitochondrial Dysfunction of DRG Neurons in DPN Mice by Targeting GPR40

DRG neurons in DPN mice (STZ, *db/db*) exhibited lower levels of oxygen consumption rate (OCR), while AB improved all above mitochondrial bioenergetics in DPN mice (Fig. 5*A–D*). Additionally, we determined that AB promoted the mitochondrial membrane potential (MMP) level of DRG neurons in DPN mice (Supplementary Fig. 4*A* and *B*). Notably, AB had no effects on the above-mentioned parameters of mitochondrial function of DRG neurons in AAV8-*GPR40-RNAi*–injected DPN mice (Fig. 5*E* and *F* and Supplementary Fig. 4*C*).

AB Ameliorated Mitochondrial Function-Related Proteins of DRG and SN Tissues in DPN Mice by Targeting GPR40

Next, we detected the regulation of AB against NDUFS3 and COX IV in DRG and SN tissues of DPN mice. The results indicated that AB upregulated the levels of these two proteins in the DRG and SN tissues of DPN mice (STZ, *db/db*) (Fig. 5*G–J* and Supplementary Fig. 4*D–G*), but had no impacts on either of these two proteins in AAV8-*GPR40-RNAi*–injected DPN mice (Fig. 5*K* and *L* and Supplementary Fig. 4*H* and *I*).

AB Improved Mitochondrial Dysfunction of DRG and SN Tissues Through the GPR40/LKB1/AMPK/SIRT1/PGC-1α Pathway in DPN Mice

Considering that the AMPK/SIRT1/PGC-1α pathway is potently involved in mitochondrial function (1,36), we detected the regulation of AB against this pathway in DPN mice. Our results indicated that AB upregulated the protein levels of phosphorylated AMPK at Thr172 site (P-AMPK), SIRT1 and PGC-1α in DRG and SN tissues of DPN mice (STZ, *db/db*) (Fig. 5*G–J* and Supplementary Fig. 4*D–G*). Notably, AB had no impacts on the AMPK/SIRT1/PGC-1α pathway in AAV8-*GPR40-RNAi*–injected DPN mice (Fig. 5*K* and *L* and Supplementary Fig. 4*H* and *I*).

Both CAMKKβ and LKB1 can regulate AMPK (37,38), and our results demonstrated that AB had no impacts on CAMKKβ protein level (Supplementary Fig. 4*J* and *K*) but upregulated the LKB1 protein level (Fig. 5*G–J* and Supplementary Fig. 4*D–G*). We thus suggested that AB improved mitochondrial dysfunction of DRG and SN tissues through the GPR40/LKB1/AMPK/SIRT1/PGC-1α pathway in DPN mice by targeting GPR40.

AB Protected Against DRG Neurons Apoptosis in DPN Mice by Targeting GPR40

TUNEL assay results demonstrated that the apoptosis of DRG neurons in DPN mice (STZ, *db/db*) was worsened (Fig. 5*M–P*) and that AB repressed apoptosis of DRG neurons in DPN mice. Notably, AB lost such a repressive capability in AAV8-*GPR40-RNAi*–injected DPN mice (Fig. 5*Q* and *R*). All results indicated that AB protected against DRG neuronal apoptosis in DPN mice by targeting GPR40.

AB Enhanced Neurite Outgrowth of DRG Neurons in DPN Mice by Targeting GPR40

Axonal damage and DRG neuronal injury are tightly connected with DPN (1), and our results demonstrated that AB enhanced the neurite outgrowth of DRG neurons in DPN mice (Supplementary Fig. 4*L–O*) but lost such a beneficial effect in AAV8-*GPR40-RNAi*–injected DPN mice

respiration capacity in DRG neurons from AAV8-*GPR40-RNAi*–injected STZ mice ($n = 4$). Western blot with quantification results demonstrated that AB (2 or 4 mg/kg/day) upregulated the expression of LKB1, P-AMPK, SIRT1, PGC-1α, NDUFS3, and COX IV in DRG neurons from DPN mice (STZ, $n = 3$; *db/db*, $n = 3$) (*G–J*), while AB (4 mg/kg/day) had no impacts on LKB1/AMPK/SIRT1/PGC-1α signaling pathway in the AAV8-*GPR40 RNAi*–injected STZ mice ($n = 3$) (*K* and *L*). T-AMPK, total AMPK. Immunofluorescence (Neu N-labeled DRG neurons, green; TUNEL-labeled apoptosis cells, red) with quantification results demonstrated that AB (2, 4 mg/kg/day) suppressed the apoptosis of DRG neurons from DPN mice (STZ, $n = 3$; *db/db*, $n = 3$) (*M–P*), while AB (4 mg/kg/day) had no impacts on DRG neuronal apoptosis in AAV8-*GPR40-RNAi*–injected STZ mice ($n = 3$) (*Q* and *R*). All values are presented as mean ± SEM. $^*P < 0.05$, $^{**}P < 0.01$, $^{***}P < 0.001$ vs. control or *db/m* mice; ns, not significant; one-way ANOVA with the Dunnett post hoc test.

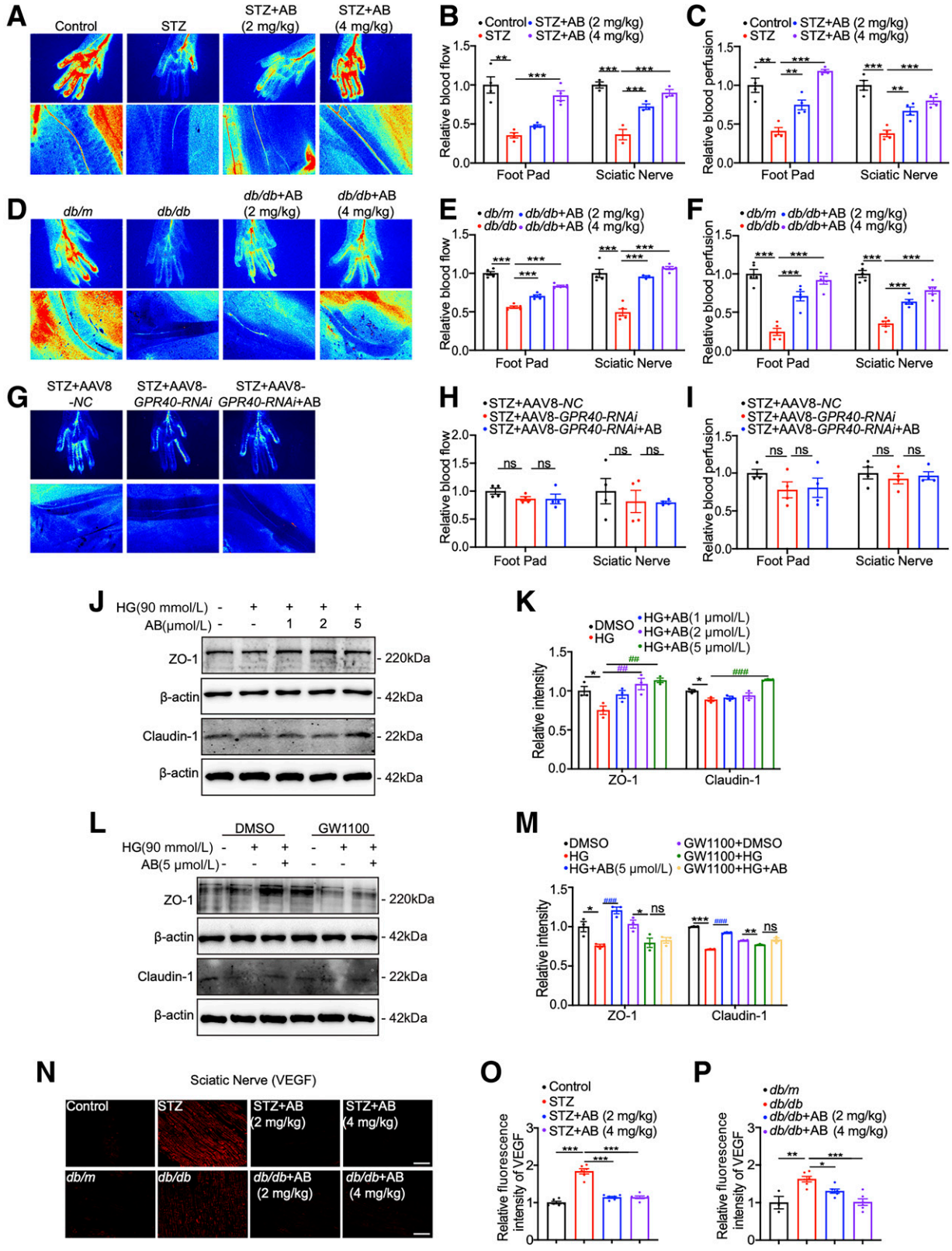

Figure 6—AB improved peripheral vascular dysfunction and endothelial permeability disorder in DPN mice by targeting GPR40. *A*: Representative images with quantification results revealed that AB (2 or 4 mg/kg/day) increased blood flow velocities (*B*) and regional blood perfusion areas (*C*) of foot pads and sciatic nerves in STZ mice (n = 4). *D*: Representative images with quantification results revealed that AB (2 or 4 mg/kg/day) increased blood flow velocities (*E*) and regional blood perfusion areas (*F*) of foot pads and SNs in *db*/*db* mice (n = 5). *G*: Representative images with quantification results revealed that AB (4 mg/kg/day) lost its enhancive capability in blood flow velocities (*H*) and regional blood perfusion areas (*I*) of foot pads and SNs in the AAV8-*GPR40-RNAi*–injected STZ mice (n = 4). Flow velocity and perfusion

(Supplementary Fig. 4*P* and *Q*). These results implied that AB enhanced neurite outgrowth of DRG neurons in DPN mice by targeting GPR40.

Collectively, all results demonstrated that AB protected against DRG neuronal apoptosis and mitochondrial dysfunction in DPN mice through the GPR40/LKB1/AMPK/SIRT1/PGC-1α signaling pathway.

AB Improved Peripheral Vascular Dysfunction and Endothelial Permeability Disorder in DPN Mice by Targeting GPR40

AB Improved Peripheral Vascular Dysfunction in DPN Mice by Targeting GPR40

Concerning that microvascular damage is a key to DPN pathology (39), we examined the beneficial effect of AB on vascular dysfunction by detecting the blood flow velocity and blood perfusion area in SNs and foot pads of DPN mice. The results indicated that both blood flow velocity and blood perfusion areas were suppressed in DPN mice (STZ, *db/db*) but promoted in the AB-treated DPN mice (Fig. 6*A–F*). Notably, AB had no impacts on either of these two items in AAV8-*GPR40-RNAi*–injected DPN mice (Fig. 6*G–I*).

AB Improved Endothelial Permeability Disorder in Human Umbilical Vein Endothelial Cells by Targeting GPR40

SNs are composed of nerve fibers and surrounded with epineurium and endoneurium, while peripheral nerve function is affected by its associated blood vessels (40). Additionally, the downregulation of tight junction proteins ZO-1 and claudin-1 denotes the impaired vascular permeability in endothelial cells (41). With these facts, our results indicated that AB antagonized the decreases in the protein levels of ZO-1 and claudin-1 (Fig. 6*J* and *K*) and that GW1100 deprived AB of its antagonistic activity in HG-induced human umbilical vein endothelial cells (HUVEC) (Fig. 6*L* and *M*), which demonstrated that AB improved endothelial permeability by targeting GPR40.

AB Improved Endothelial Permeability Disorder of SN Tissues in DPN Mice by Targeting GPR40

Moreover, immunofluorescence results demonstrated that the protein level of vascular endothelial growth factor was upregulated, but ZO-1 and claudin-1 were both downregulated in the SN tissues of DPN mice (STZ, *db/db*), while AB ameliorated the above-mentioned vascular impairments in DPN mice (Fig. 6*N–P* and Supplementary Fig. 5*A–F*). Notably, AB had no impacts on those proteins in AAV8-*GPR40-RNAi*–injected DPN mice (Supplementary Fig. 5*G* and *H*).

All results implied that AB improved peripheral vascular dysfunction and neurovascular endothelial permeability disorder in DPN mice by targeting GPR40.

AB Improved Endothelial Permeability Disorder and Mitochondrial Dysfunction by Suppressing Neuroinflammation

We next focused on the endothelial-related cross talk to investigate the potential of AB in ameliorating DPN-like pathology by conditioned medium assay (42) (Fig. 7*A*).

AB Ameliorated Endothelial Permeability Disorder Involving Schwann Cells/HUVEC Cells Cross Talk

Western blot results indicated that the conditioned medium with activated NLRP3 inflammasome from LPS/ATP-treated RSC96 cells (Fig. 4*A*) caused the suppression of ZO-1 and claudin-1, while AB antagonized such a suppression in HUVEC cells (Fig. 7*B* and *C*). However, the conditioned medium from HG-treated HUVEC cells (Fig. 6*J*) failed to activate NLRP3 inflammasome in RSC96 cells (Supplementary Fig. 6*A* and *B*). These results implied that endothelial and epineural permeability damage was attributed to the inflammatory reaction of Schwann cells.

AB Ameliorated Mitochondrial Dysfunction Involving Schwann Cells/DRG Neurons Cross Talk

Given that mitochondrial damage in Schwann cells and DRG neurons is tightly associated with DPN pathology (43), the conditioned medium-based assays were performed (Fig. 7*D*). Western blot results indicated that the conditioned medium from the LPS/ATP-treated RSC96 cells caused the suppression of NDUFS3 and COX IV, but AB antagonized this inhibition in primary DRG neurons (Fig. 7*E* and *F*). In addition, TUNEL assay results indicated that AB efficiently protected against DRG neuronal apoptosis induced by the conditioned medium from LPS/ATP-treated RSC96 cells (Fig. 7*G* and *H*). Similarly, the conditioned medium from DRG neurons failed to activate NLRP3 inflammasome in RSC96 cells (Supplementary Fig. 6*E* and *F*). These results suggested that mitochondrial dysfunction of DRG neurons was caused by the inflammatory reaction of Schwann cells and that mitochondrial dysfunction was not sufficient to cause inflammation.

Taken together, all results implied that AB ameliorated endothelial permeability and mitochondrial dysfunction by suppressing neuroinflammation.

area are shown as different colors in blue, green, yellow-orange, and red as represented from low to high. All values are presented as mean ± SEM. $*P < 0.05$, $**P < 0.01$, $***P < 0.001$; ns, not significant; one-way ANOVA with the Dunnett post hoc test. Western blot with quantification results demonstrated that AB (1, 2, or 5 μmol/L) increased the expression of ZO-1 and claudin-1 (*J* and *K*) and that GW1100 (10 μmol/L) suppressed this ameliorative effect of AB (5 μmol/L) in the HG (90 mmol/L)-treated HUVEC cells ($n = 3$) (*L* and *M*). All values are presented as mean ± SEM. $*P < 0.05$, $**P < 0.01$, $***P < 0.001$; $\#\#P < 0.01$, $\#\#\#P < 0.001$ vs. HG; one-way ANOVA with the Dunnett post hoc test. *N–P*: Immunofluorescence with quantification results suggested that AB (2 or 4 mg/kg/day) antagonized the upregulation of protein level of vascular endothelial growth factor (VEGF) (red) in SNs from DPN mice (STZ, $n = 5$; *db/db*, $n = 5$). Scale bar: 25 μm. All values are presented as mean ± SEM. $*P < 0.05$, $**P < 0.01$, $***P < 0.001$ vs. control or *db/m* mice; ns, not significant; one-way ANOVA with the Dunnett post hoc test.

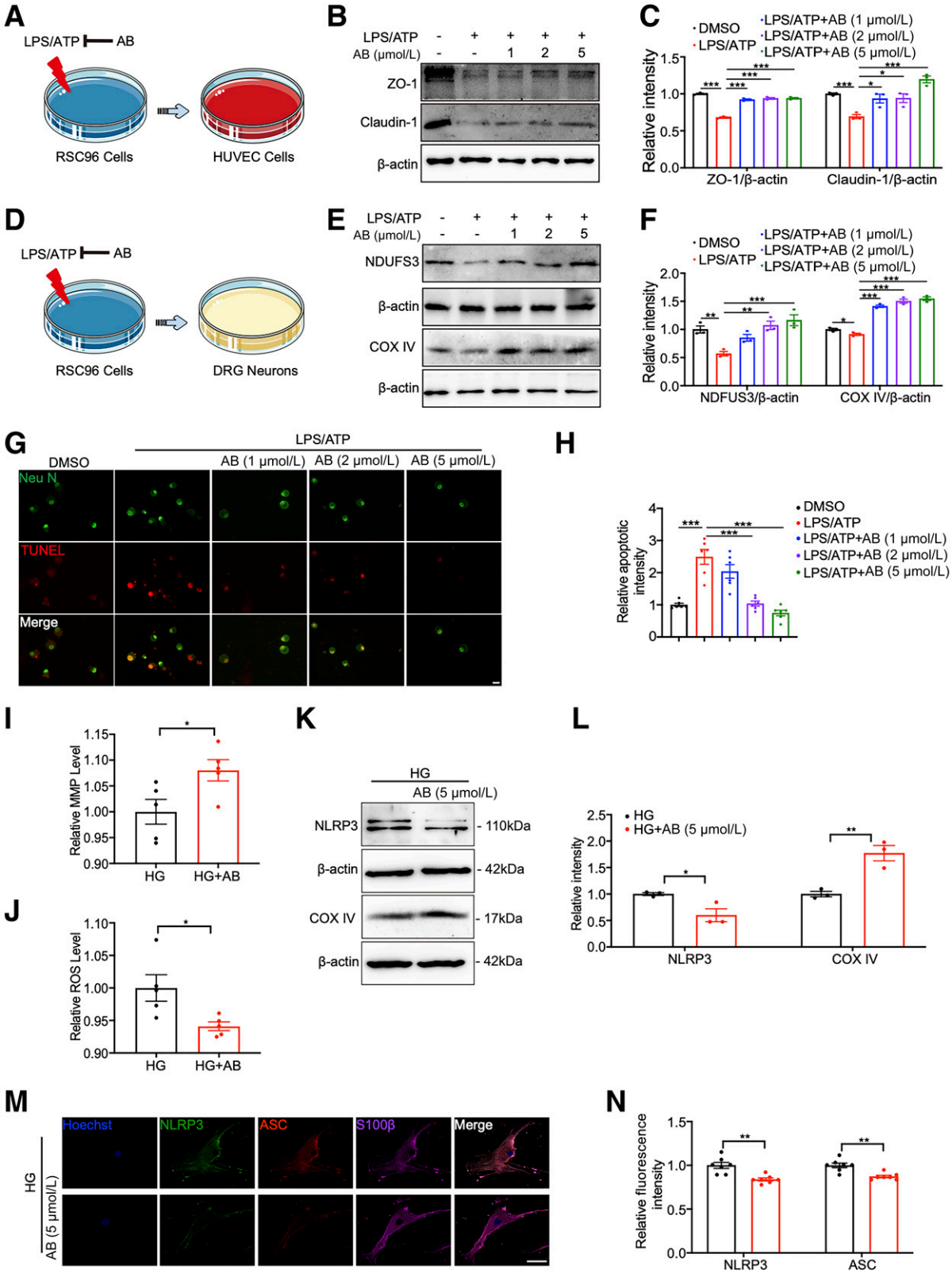

Figure 7—AB ameliorated mitochondrial dysfunction and inflammation in HSCs. *A*: Schematic diagram of conditional medium experiments in RSC96 and HUVEC cells. *B* and *C*: Western blot with quantification results demonstrated that AB (1, 2, or 5 μmol/L) increased the expression levels of ZO-1 and claudin-1 in the conditional medium-treated DRG neurons (n = 3). *D*: Schematic diagram of the conditional medium experiments in RSC96 cells and primary DRG neurons. *E* and *F*: Western blot with quantification results demonstrated that AB (1, 2, or 5 μmol/L) increased the protein levels of NDUFS3 and COX IV in the conditional medium-treated DRG neurons (n = 3). *G* and *H*: Immunofluorescence images (Neu N-labeled DRG neurons, green; TUNEL-labeled apoptosis cells, red) with quantification

AB Ameliorated Mitochondrial Dysfunction and Inflammation in Human Schwann Cells via GPR40

Since AB has been confirmed to exhibit effects of mitochondrial protection and anti-inflammation in DPN mice, we verified such beneficial effects of AB in primary human Schwann cells (HSCs) that were extracted from sciatic nerves of DPN patients (No. CHEC2023-088) (The cells were identified with S100β; HG was used for maintaining hyperglycemia) (Supplementary Fig. 6*G*).

As indicated in Fig. 7*I–N* and Supplementary Fig. 6*H* and *I*, AB inhibited inflammation by suppression of NLRP3 and ASC protein levels and enhanced mitochondrial function by regulating reactive oxygen species, MMP levels, and promotion of protein levels of NDUFS3 and COX IV, while GPR40 inhibitor GW1100 deprived AB of its above capabilities in HSCs (Supplementary Fig. 6*J–L*). These results thus demonstrated that AB exerted these effects in HSCs by targeting GPR40.

All results verified that AB ameliorated neuroinflammation and mitochondrial dysfunction via GPR40 in HSCs.

DISCUSSION

DPN is a severe diabetes complication that can progress to diabetic foot ulcers, significantly increasing the risk of limb amputation and mortality. Owing to the limited understanding of the complicated pathological mechanisms underlying DPN, the development of effective therapeutic interventions has remained a significant challenge.

In our previous work, we identified an abnormal reduction in GPR40 protein expression in DPN mice (12) and SN tissues of DPN patients. This finding led us to hypothesize that GPR40 may play a critical role in the regulation of the pathogenesis of DPN.

In the current work, we demonstrated that AB is a GPR40 agonist and effectively alleviates DPN-like pathology in mice. Notably, AB is a clinically approved drug for the treatment of hypertension, coronary heart disease, and angina. Epidemiological studies have revealed a strong coexistence of essential hypertension and diabetes, with DPN patients often exhibiting higher blood pressure variability compared with individuals without diabetes (44). To our knowledge, our study might be the first to reveal that AB can improve DPN through pharmacological mechanisms distinct from its antihypertensive effects. This discovery highlights the potential for AB to serve a dual therapeutic purpose—effectively addressing both hypertension and DPN in patients—thereby embodying the concept of "killing two birds with one stone."

Inflammation and mitochondrial dysfunction are integral to the entire progression of DPN and serve as critical pathological factors contributing nerve function impairment and neuronal apoptosis (33,45). Elevated levels of abnormal cytokines, increased infiltration of peripheral neuroinflammatory cells, and alterations in bone marrow-derived in proinflammatory factors are all closely associated with the inflammatory response. Concurrently, mitochondrial dysfunction exacerbates neuronal apoptosis (45,46). In this context, the NLRP3 inflammasome plays a pivotal role in regulating inflammation, while β-arrestin2, a downstream scaffold protein of GPR40, is also intimately linked to inflammatory processes (35). Our findings demonstrated that AB exhibits its therapeutic effects by modulating two pathways: *1*) the GPR40/β-arrestin2/NLRP3 pathway, through which it suppresses the inflammatory response, and *2*) the GPR40/LKB1/AMPK/SIRT1/PGC-1α pathway, which enhances mitochondrial function. Furthermore, DPN pathology is characterized by impaired blood flow and increased neurovascular endothelial permeability, both of which ultimately contribute to peripheral neuronal dysfunction (47). AB, by targeting GPR40, effectively ameliorates peripheral neurovascular dysfunction and restores vascular endothelial permeability in DPN mice. Collectively, these findings provide a potent foundation for elucidating the mechanisms underlying the protective effects of AB on the peripheral neuronal damage.

As the main glial cells of the peripheral nervous system, Schwann cells play a crucial role in maintaining neuronal homeostasis and supporting peripheral nerve nutrition, while serving as the primary responders to neural injury (48). In the pathological state, Schwann cells produce an inflammatory response and release proinflammatory cytokines that affect peripheral cell function (49). We validated the interaction of endothelial cells with Schwann cells at the cellular level through the conditioned medium experiments and highlighted the fact that the damage of vascular endothelial cells is induced by the inflammatory factors from the Schwann cells.

Given the anatomical arrangement where SNs are enveloped by Schwann cells and extend to the dorsal root to provide essential nutrients for axonal growth of DRG neurons (50), we here conducted a series of conditioned medium-based experiments to investigate the Schwann cells/DRG neurons interactions. Our results demonstrate that Schwann cells activation and subsequent release of inflammatory factors serve as key mediators triggering mitochondrial dysfunction in DRG neurons.

results demonstrated that AB (1, 2, or 5 μmol/L) suppressed the conditioned medium-induced apoptosis in DRG neurons ($n = 6$). Scale bar: 100 μm. All values are presented as mean ± SEM. *$P < 0.05$, **$P < 0.01$, ***$P < 0.001$; one-way ANOVA with the Dunnett post hoc test. *I*: AB (5 μmol/L) improved the mitochondrial membrane potential level in HSCs ($n = 5$). *J*: AB (5 μmol/L) downregulated reactive oxygen species (ROS) level in HSCs ($n = 5$). *K* and *L*: Western blot with quantification results demonstrated that AB (5 μmol/L) repressed NLRP3 protein level and upregulated COX IV protein level in HSCs ($n = 3$). *M* and *N*: Immunofluorescence (NLRP3, green; ASC, red; S100β, purple) with quantification results demonstrated that AB (5 μmol/L) suppressed NLRP3 inflammasome activation in HSCs ($n = 7$).

In conclusion, our study demonstrates that AB functions as a potent GPR40 agonist to ameliorate DPN-like pathology in mice. Mechanistically, AB exerts its therapeutic effects through dual pathways: *1*) suppression of inflammatory responses via the GPR40/β-arrestin2/NLRP3 pathway, and *2*) improvement of mitochondrial dysfunction through the GPR40/LKB1/AMPK/SIRT1/PGC-1α axis. These mechanisms were consistently observed in both DPN model mice and primary HSCs. Furthermore, AB effectively attenuated the pathological cross talk between Schwann cells and endothelial cells/DRG neurons. Collectively, our findings strongly support the therapeutic potential of AB as a promising candidate for DPN treatment.

Funding. This work was supported by the National Natural Science Foundation of China (82473982, 81930057), Innovation Projects of State Key Laboratory on Technologies for Chinese Medicine Pharmaceutical Process Control and Intelligent Manufacture (no. NZYSKL240110), Major Program of the Natural Science Foundation of the Jiangsu Higher Education Institutions of China (23KJA350002), and "Qing Lan" project, Shanghai Rising-Star Program (Sailing Special Program) (23YF1458400), and Shanghai excellent academic leader (23XD1425000).

Duality of Interest. No potential conflicts of interest relevant to this article were reported.

Author Contributions. Y.W. performed research and analyzed data. Y.W. wrote the manuscript. Y.H. and R.H. contributed reagents. Y.R., T.F., F.Z., W.Z., J.L., S.X., and Y.Y. undertook clinical assessments. J.W., S.J., and X.S. designed research. J.W. and X.S. reviewed the manuscript. J.W. and X.S. are the guarantors of this work and, as such, had full access to all the data in the study and take responsibility for the integrity of the data and the accuracy of the data analysis.

References

1. Xu X, Wang W, Wang Z, et al. DW14006 as a direct AMPKα activator ameliorates diabetic peripheral neuropathy in mice. Diabetes 2020;69:1974–1988
2. Feldman EL, Nave K-A, Jensen TS, Bennett DLH. New horizons in diabetic neuropathy: mechanisms, bioenergetics, and pain. Neuron 2017;93:1296–1313
3. Wang C-S, Pai Y-W, Lin C-H, Lee I-T, Chen H-H, Chang M-H. Diabetic peripheral neuropathy: age-stratified glycemic control. Front Endocrinol (Lausanne) 2024;15:1377923–1377929
4. Calcutt NA. Diabetic neuropathy and neuropathic pain: a (con)fusion of pathogenic mechanisms? Pain 2020;161:S65–S86
5. Qiang X, Satoh J, Sagara M, et al. Inhibitory effect of troglitazone on diabetic neuropathy in streptozotocin-induced diabetic rats. Diabetologia 1998; 41:1321–1326
6. Luo Q, Feng Y, Xie Y, et al. Nanoparticle-microRNA-146a-5p polyplexes ameliorate diabetic peripheral neuropathy by modulating inflammation and apoptosis. Nanomedicine 2019;17:188–197
7. Fan J, Pan Q, Gao Q, Li W, Xiao F, Guo L. TSH combined with TSHR aggravates diabetic peripheral neuropathy by promoting oxidative stress and apoptosis in Schwann cells. Oxid Med Cell Longev 2021;2021:2482453–2482475
8. Ben Y, Hao J, Zhang Z, et al. Astragaloside IV inhibits mitochondrial-dependent apoptosis of the dorsal root ganglion in diabetic peripheral neuropathy rats through modulation of the SIRT1/p53 signaling pathway. Diabetes Metab Syndr Obes 2021;14:1647–1661
9. Roy Chowdhury SK, Smith DR, Saleh A, et al. Impaired adenosine monophosphate-activated protein kinase signalling in dorsal root ganglia neurons is linked to mitochondrial dysfunction and peripheral neuropathy in diabetes. Brain 2012;135:1751–1766
10. Fan B, Li C, Szalad A, et al. Mesenchymal stromal cell-derived exosomes ameliorate peripheral neuropathy in a mouse model of diabetes. Diabetologia 2020;63:431–443
11. Engel DF, Bobbo VCD, Solon CS, et al. Activation of GPR40 induces hypothalamic neurogenesis through p38- and BDNF-dependent mechanisms. Sci Rep 2020;10:11047–11058
12. Xu J-W, Xu X, Ling Y, et al. Vincamine as an agonist of G-protein-coupled receptor 40 effectively ameliorates diabetic peripheral neuropathy in mice. Acta Pharmacol Sin 2023;44:2388–2403
13. Xiao J, Cai T, Fang Y, et al. Activation of GPR40 attenuates neuroinflammation and improves neurological function via PAK4/CREB/KDM6B pathway in an experimental GMH rat model. J Neuroinflammation 2021;18:160–175
14. Ha T-Y, Kim J-B, Kim Y, Park SM, Chang K-A. GPR40 agonist ameliorates neurodegeneration and motor impairment by regulating NLRP3 inflammasome in Parkinson's disease animal models. Pharmacol Res 2024;209:107432
15. Jabůrek M, Klöppel E, Průchová P, et al. Mitochondria to plasma membrane redox signaling is essential for fatty acid β-oxidation-driven insulin secretion. Redox Biol 2024;75:103283–103219
16. Lei L, Gao X, Zhai J, et al. The GPR40 novel agonist SZZ15-11 improves non-alcoholic fatty liver disease by activating the AMPK pathway and restores metabolic homeostasis in diet-induced obese mice. Diabetes Obes Metab 2024;26:2257–2266
17. Sloan G, Selvarajah D, Tesfaye S. Pathogenesis, diagnosis and clinical management of diabetic sensorimotor peripheral neuropathy. Nat Rev Endocrinol 2021;17:400–420
18. Du T, Yang L, Xu X, et al. Vincamine as a GPR40 agonist improves glucose homeostasis in type 2 diabetic mice. J Endocrinol 2019;240:195–214
19. Huang Y, Ren H, Gao X, et al. Amlodipine improves spinal cord injury repair by inhibiting motoneuronal apoptosis through autophagy upregulation. Spine (Phila Pa 1976) 2022;47:E570–E578
20. Lee YJ, Park H-H, Koh S-H, Choi N-Y, Lee K-Y. Amlodipine besylate and amlodipine camsylate prevent cortical neuronal cell death induced by oxidative stress. J Neurochem 2011;119:1262–1270
21. Li Y, Zhao D, Qian M, et al. Amlodipine, an anti-hypertensive drug, alleviates non-alcoholic fatty liver disease by modulating gut microbiota. Br J Pharmacol 2022;179:2054–2077
22. Cserép C, Pósfai B, Dénes Á. Shaping neuronal fate: functional heterogeneity of direct microglia-neuron interactions. Neuron 2021;109:222–240
23. Zhou H, Yang X, Liao C, et al. The development of mechanical allodynia in diabetic rats revealed by single-cell RNA-Seq. Front Mol Neurosci 2022;15: 856213–856299
24. Pacifico P, Coy-Dibley JS, Miller RJ, Menichella DM. Peripheral mechanisms of peripheral neuropathic pain. Front Mol Neurosci 2023;16: 1252415–1252442
25. Wang Y, Guo L, Yin X, et al. Pathogenic TNF-α drives peripheral nerve inflammation in an Aire-deficient model of autoimmunity. Proc Natl Acad Sci U S A 2022;119:e2114406119
26. Eid SA, Noureldein M, Kim B, et al. Single-cell RNA-seq uncovers novel metabolic functions of Schwann cells beyond myelination. J Neurochem 2023;166:367–388
27. Cheng HT, Dauch JR, Hayes JM, Hong Y, Feldman EL. Nerve growth factor mediates mechanical allodynia in a mouse model of type 2 diabetes. J Neuropathol Exp Neurol 2009;68:1229–1243
28. Hur J, Dauch JR, Hinder LM, et al. The metabolic syndrome and microvascular complications in a murine model of type 2 diabetes. Diabetes 2015;64:3294–3304
29. Zherebitskaya E, Akude E, Smith DR, Fernyhough P. Development of selective axonopathy in adult sensory neurons isolated from diabetic rats: role of glucose-induced oxidative stress. Diabetes 2009;58:1356–1364
30. Herbert AL, Fu M-M, Drerup CM, et al. Dynein/dynactin is necessary for anterograde transport of Mbp mRNA in oligodendrocytes and for myelination in vivo. Proc Natl Acad Sci U S A 2017;114:E9153–E9162

31. Li P, Chen C, Huang B, Jiang Z, Wei J, Zeng J. Altered excitability of motor neuron pathways after stroke: more than upper motor neuron impairments. Stroke Vasc Neurol 2022;7:518–526
32. Wang Q, Li H-Y, Ling Z-M, Chen G, Wei Z-Y. Inhibition of Schwann cell pannexin 1 attenuates neuropathic pain through the suppression of inflammatory responses. J Neuroinflammation 2022;19:244
33. Zhou R, Yazdi AS, Menu P, Tschopp J. A role for mitochondria in NLRP3 inflammasome activation. Nature 2011;469:221–225
34. Zhang D, Jing B, Chen Z-N, et al. Ferulic acid alleviates sciatica by inhibiting neuroinflammation and promoting nerve repair via the TLR4/NF-κB pathway. CNS Neurosci Ther 2023;29:1000–1011
35. Lin C, Chao H, Li Z, et al. Omega-3 fatty acids regulate NLRP3 inflammasome activation and prevent behavior deficits after traumatic brain injury. Exp Neurol 2017;290:115–122
36. Zhang Q, Song W, Zhao B, et al. Quercetin attenuates diabetic peripheral neuropathy by correcting mitochondrial abnormality via activation of AMPK/PGC-1α pathway in vivo and in vitro. Front Neurosci 2021;15:636172–636187
37. Hou L, Jiang F, Huang B, et al. Dihydromyricetin resists inflammation-induced muscle atrophy via ryanodine receptor-CaMKK-AMPK signal pathway. J Cell Mol Med 2021;25:9953–9971
38. Eom J-W, Lee J-M, Koh J-Y, Kim Y-H. AMP-activated protein kinase contributes to zinc-induced neuronal death via activation by LKB1 and induction of Bim in mouse cortical cultures. Mol Brain 2016;9:14–26
39. Jin HY, Joung SJ, Park JH, Baek HS, Park TS. The effect of alpha-lipoic acid on symptoms and skin blood flow in diabetic neuropathy. Diabet Med 2007;24:1034–1038
40. Samii A, Unger J, Lange W. Vascular endothelial growth factor expression in peripheral nerves and dorsal root ganglia in diabetic neuropathy in rats. Neurosci Lett 1999;262:159–162
41. Königs V, Pierre S, Schicht M, et al. GPR40 activation abolishes diabetes-induced painful neuropathy by suppressing VEGF-A expression. Diabetes 2022;71:774–787
42. Cho YR, Lim JH, Kim MY, et al. Therapeutic effects of fenofibrate on diabetic peripheral neuropathy by improving endothelial and neural survival in *db*/*db* mice. PLoS One 2014;9:e83204
43. Zhang L, Zhao H, Blagg BSJ, Dobrowsky RT. C-terminal heat shock protein 90 inhibitor decreases hyperglycemia-induced oxidative stress and improves mitochondrial bioenergetics in sensory neurons. J Proteome Res 2012;11:2581–2593
44. Grossman A, Grossman E. Blood pressure control in type 2 diabetic patients. Cardiovasc Diabetol 2017;16:3–17
45. Yerra VG, Kalvala AK, Kumar A. Isoliquiritigenin reduces oxidative damage and alleviates mitochondrial impairment by SIRT1 activation in experimental diabetic neuropathy. J Nutr Biochem 2017;47:41–52
46. Ni G-L, Cui R, Shao A-M, Wu Z-M. Salidroside ameliorates diabetic neuropathic pain in rats by inhibiting neuroinflammation. J Mol Neurosci 2017;63:9–16
47. Tan J-S, Lin C-C, Chen G-S. Vasomodulation of peripheral blood flow by focused ultrasound potentiates improvement of diabetic neuropathy. BMJ Open Diabetes Res Care 2020;8:1136–1144
48. Yadav A, Huang T-C, Chen S-H, et al. Sodium phenylbutyrate inhibits Schwann cell inflammation via HDAC and NFκB to promote axonal regeneration and remyelination. J Neuroinflammation 2021;18:238–254
49. Fumagalli G, Monza L, Cavaletti G, Rigolio R, Meregalli C. Neuroinflammatory process involved in different preclinical models of chemotherapy-induced peripheral neuropathy. Front Immunol 2020;11:626624–626687
50. Enamorado M, Kulalert W, Han S-J, et al. Immunity to the microbiota promotes sensory neuron regeneration. Cell 2023;186:607–620.e17